Three-body continuum-discretized coupled-channel calculations for ^{6}He scattering from heavy nuclei

K. Rusek,[1] I. Martel,[1] J. Gómez-Camacho,[2] A. M. Moro,[2] and R. Raabe[3]

[1]*Departamento de Física Aplicada, Universidad de Huelva, E-21819, Huelva, Spain*
[2]*Departamento de Física Atómica, Molecular y Nuclear, Universidad de Sevilla, Apartado 1065, E-41080 Sevilla, Spain*
[3]*Instituut voor Kern- en Stralingsfysica, Katholieke Universiteit Leuven, Celestijnenlaan 200D, B-3001 Leuven, Belgium*

Data for scattering of ^{6}He from ^{197}Au, ^{208}Pb, and ^{209}Bi targets at low energies were consistently analyzed by use of the continuum-discretized coupled-channels method and the dineutron model of the projectile. A very good description of the experimental data was obtained with the strength of the dipole couplings reduced by 50%. We find that the dipole couplings are responsible for the suppression of the Coulomb rainbow and that the quadrupole couplings must be included in the calculations in order to obtain good agreement with the elastic-scattering data at more backward angles.

PACS number(s): 25.60.Bx, 24.10.Eq, 21.60.Gx

The continuum-discretized coupled-channel (CDCC) method, developed originally to study the effect of deuteron breakup on the process of elastic scattering [1], plays an important role in the study of reactions with weakly bound light nuclei. So far the method has been limited to the three-body systems, allowing the study of interactions of a projectile consisting of two clusters with a target nucleus. Some efforts have been reported recently to extend it to the four-body systems [2–4] so that the scattering of ^{6}He, the nucleus known to have a three-body $\alpha + n + n$ structure, could be studied. However, these approaches are not applicable yet for the processes taking place in the vicinity of the Coulomb barrier because they do not account for the four-body Coulomb breakup of the projectile.

Therefore low-energy ^{6}He elastic-scattering data have been analyzed so far by use of the limited model of this nucleus, with the two neutrons outside the α-particle core coupled to a single particle, a dineutron (^2n), [5,6]. For ^{6}He scattered from ^{208}Pb at a laboratory energy of 29.6 MeV, the CDCC calculations reproduced well the measured angular distribution of elastically scattered ^{6}He [5] whereas similar calculations for the ^{209}Bi target were unable to describe the elastic-scattering angular distributions measured at bombarding energies of 19 and 22.5 MeV [6].

New, much more precise data for ^{6}He scattered from ^{208}Pb [7] published recently as well as data for a ^{197}Au target measured at the Cyclotron Research Centre in Louvain-la-Neuve open the possibility for more detailed studies of the applicability of such a simplified approach. The experiment at Louvain-la-Neuve was part of a campaign (by the PH-114 collaboration [8,9]) in which scattering of ^{6}He by different targets was investigated; details are given in Ref. [10]. In this report we present results of CDCC calculations limited to the three-body systems for these data sets.

The calculations follow closely the procedure of Keeley *et al.* [6]. The two-body $\alpha + {}^2n$ model of ^{6}He was employed, with the spin of the dineutron cluster set to zero. The potential binding the two clusters was of Woods-Saxon form, with the set II parameters listed in Table I of Ref. [11]. All

the interactions were derived from empirical optical-model potentials describing elastic scattering of α particles and deuterons from the gold and lead targets [12,13] by use of the single-folding technique. The calculations were performed by means of the computer code FRESCO, version frxp18 [14].

The continuum of the $\alpha + {}^2n$ cluster states was truncated at relative momentum $k = 0.6$ fm^{-1} and discretized into bins of $\Delta k = 0.1$ fm^{-1}. The relative angular momentum of the cluster states was limited to the values $L = 0,1,2$. For the $L = 2$ states the binning scheme was modified because of the presence of the resonant state at an excitation energy of 0.825 MeV above the breakup threshold. This state was treated as a bin of width 0.3 MeV.

It has been shown that dipole polarizability of ^{6}He (dipole couplings between the ^{6}He ground state and the states from the continuum) plays a very important role at energies close to the Coulomb barrier [5]. The $E1$ coupling strength calculated by means of the dineutron model within the excitation energy range of 0–5.6 MeV is significantly larger than the experimental value reported by Aumann *et al.* [15] or predicted by the three-body $\alpha + n + n$ model of ^{6}He [16] in the similar energy range [Fig. 1(a)]. This suggests that the dineutron model overestimates the effect of ^{6}He polarizability. To study this problem a series of test calculations was performed for the ^{6}He + ^{208}Pb system with the limited model space, including only the continuum of $L = 1$ states and no couplings between them. Thus the only couplings included in the calculations were the dipole couplings between the ground state ($L = 0$) of ^{6}He and the $L = 1$ states from the continuum. The results of the test calculations are plotted in Fig. 1(b). In the first calculation the dineutron model without any free parameter was employed, as in the two analyses performed previously [5,6] (dot-dashed curve). In the second calculation the spectroscopic amplitudes of the continuum states were set so that the energy distribution of $B(E1)$ calculated within the dineutron model was close to the distribution calculated within the three-body model of ^{6}He [16] (solid curve and filled circles in Fig. 1(a), respectively). This calculation predicted a lower effect of ^{6}He polarizability than the first one [solid curve in Fig. 1(b)]. The third calculation

TABLE I. Results of the CDCC calculations for different processes induced by ^{6}He.

	22.5 MeV Bi	27 MeV Pb	29 MeV Au	40 MeV Au
σ_{reac} (mb)	1182	1914	2176	3269
σ_{br} (mb)	218	282	301	327
σ_{fus} (mb)	333	939	1190	1815

was performed again with the dineutron model as in the first test but with one free parameter—a renormalization constant of the dipole couplings. It was found that when this constant is set to 0.5 the result is very close to the result of the second test calculation [dashed curve in Fig. 1(b)]. Angular distributions of the elastic-scattering cross sections as well as the total
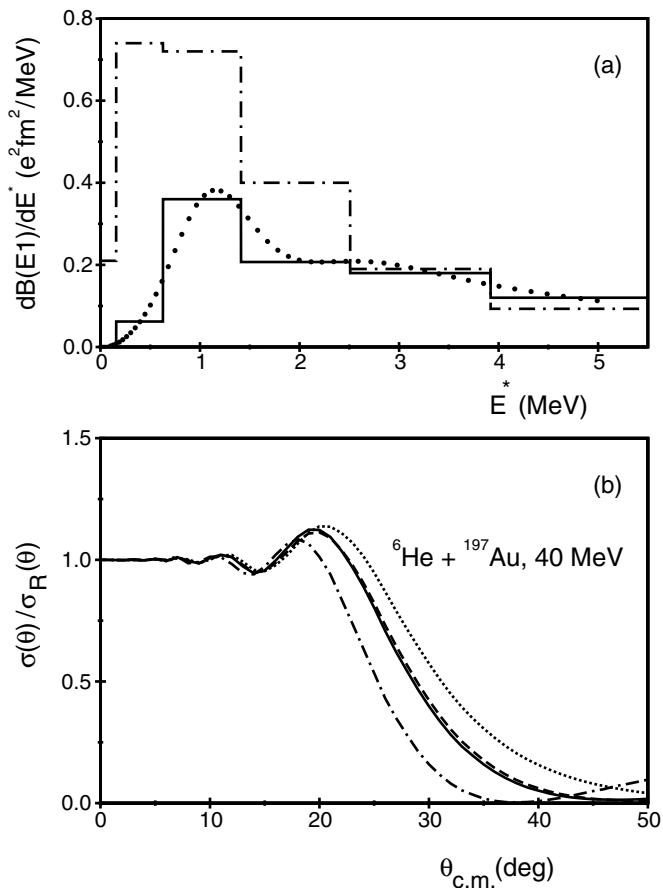

FIG. 1. (a) Energy distributions of $B(E1)$ calculated within the dineutron model: dot-dashed curve, no free parameters; solid curve, spectroscopic amplitudes of the $L = 1$ continuum states set so that the distribution is close to the one predicted by the three-body model [16] and represented by filled circles. (b) Results of the test calculations corresponding to $B(E1)$ energy distributions plotted in part (a) as well as the calculation with the dipole coupling strengths reduced by 50% (dashed curve). For comparison, the dotted curve shows the results of the one-channel calculation.
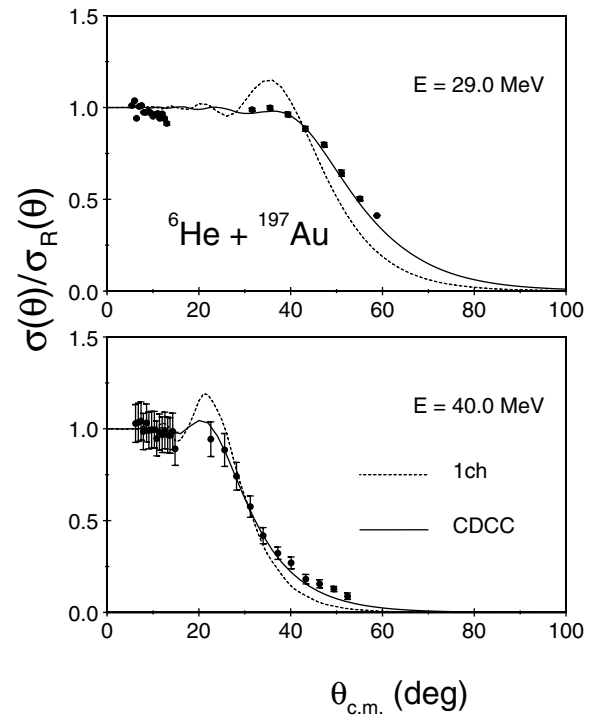

FIG. 2. Results of the calculations for the gold target. The experimental data are from Raabe [10]. Results of the one-channel calculations are plotted by the dotted curves, and the full CDCC results with reduced strength of dipole couplings are indicated by the solid curves.

reaction cross sections and breakup cross sections calculated in the latter two tests were very similar.

The test calculations suggested that, having in mind the energy distribution of $B(E1)$, one could analyze the ^{6}He scattering data by using the dineutron model either with the reduced strength of the $\lambda = 1$ couplings or with the spectroscopic amplitudes of $L = 1$ continuum states set to values different from unity. The latter method, however, would lead in the full calculation to renormalization of all the couplings, not only the dipole, with these states. Therefore our final CDCC calculations, which included couplings with the $L = 0, 1, 2$ states of the continuum, were performed with one free parameter, the renormalization constant of the dipole couplings, which was set to the value of 0.5.

The final CDCC results for ^{6}He + ^{197}Au elastic scattering at the two bombarding energies are plotted in Fig. 2 by the solid curves. The dashed curves show the results of the one-channel calculations, without coupling to the states from the ^{6}He continuum. For the two other targets, ^{208}Pb and ^{209}Bi, the results are plotted in Fig. 3. The comparison of the full CDCC calculations with the one-channel results shows that the effect of the ^{6}He breakup is significant. At the forward-scattering angles the couplings to the breakup channels reduce the characteristic oscillations of the elastic-scattering differential cross sections whereas at larger scattering angles the couplings enhance significantly the differential cross section values.

Although the effect is more pronounced at energies closer to the Coulomb barrier, the couplings mostly responsible for
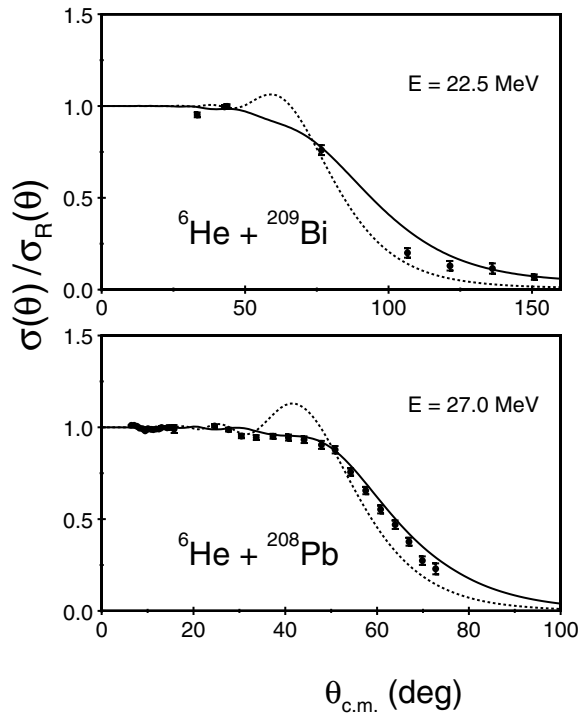
FIG. 3. As in Fig. 2 but for the lead and bismuth targets. The data are from Kakuee *et al.* [7] and Aguilera *et al.* [17], respectively.

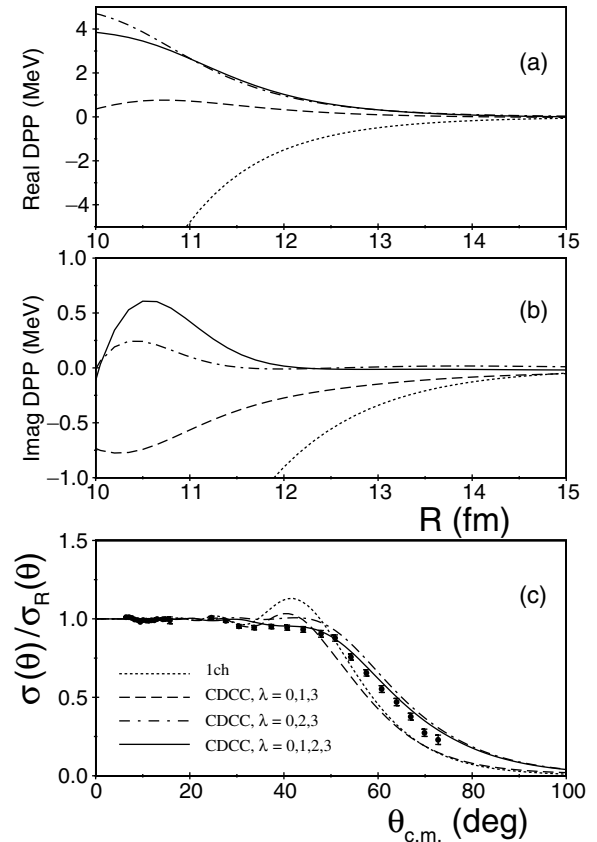
FIG. 4. Results of the calculations for ^{6}He + ^{208}Pb elastic scattering at a bombarding energy of 27 MeV. The experimental data are from Kakuee *et al.* [7]. In (c) the solid curve corresponds to the full calculation, the dashed curve to the calculation with omitted quadrupole couplings, and the dot-dashed curve to the calculation with omitted dipole couplings. In parts (a) and (b) the corresponding dynamic polarization potentials (real and imaginary components) are plotted. The dotted curves show (a) and (b) real and imaginary parts of the bare potential and (c) results of the one-channel calculations.

it are of a nuclear character. Test calculations performed for ^{6}He + ^{208}Pb at 27 MeV separately with the pure Coulomb and pure nuclear coupling potentials have shown that the calculations with the pure nuclear interactions give a result for the elastic channel that is very close to the final whereas the Coulomb component contributes mostly to the destructive interference that reduces the oscillations at forward angles.

CDCC calculations provided results also for processes other than elastic scattering. The calculated values of the total reaction cross section (σ_{reac}) as well as the cross sections for the ^{6}He $\rightarrow \alpha + ^2n$ breakup (σ_{br}) and complete fusion of the projectile with the targets (σ_{fus}), are listed in Table I. The fusion cross section was calculated by the combination of the CDCC and barrier-penetration model technique [18].

Most interesting are the results for the bismuth target, because for this target some other data rather than elastic-scattering experimental data exist. The calculated fusion cross section is in good agreement with the value of 310 ± 45 mb, measured by Kolata *et al.* [19]. Also, the total reaction cross section compares very well with the value of 1167 mb reported by Aguilera *et al.* [17]. CDCC calculations predict a relatively small cross section for ^{6}He $\rightarrow \alpha + ^2n$ breakup, much smaller than the α-production cross section measured by Aguilera *et al.* [20] (773 ± 31 mb). However, Bychowski *et al.* [20] and DeYoung *et al.* [21] have found recently that about 75% of this α-production cross section is due to the one-neutron and two-neutron transfer processes. Thus the calculated value is in agreement with the experiment. The good agreement of the CDCC calculations with the existing experimental data for ^{6}He + ^{209}Bi at 22.5 MeV suggests that a study of the role of

such direct processes like one- and two-neutron transfers, not included in the calculations, is of great interest.

Optical-model analyses of the ^{6}He elastic scattering from ^{208}Pb targets at 27 MeV have shown that, to describe the data, the central potential must include a long-range absorption term [7]. However, this long-range absorption could be only partly explained by the Coulomb dipole polarizability that was explicitly included in those analyses. To study this in more detail, we performed a series of test CDCC calculations for ^{6}He + ^{208}Pb at 27 MeV, and the results are plotted in Fig. 4(c). The dynamic polarization potentials (DPPs), generated in those calculations with the prescription of Thompson *et al.* [22] (their real and imaginary parts) are plotted in Figs. 4(a), and 4(b), respectively. The dotted curve in Fig. 4(c) shows the result of a one-channel calculation (as in Fig. 3) with the bare complex potential plotted in Figs. 4(a) and 4(b). The results of the full CDCC calculation (as in Fig. 3) as well as the DPP generated in it are represented by the solid curves. The CDCC calculation with the omitted quadrupole

couplings is indicated by the dashed curves. In this calculation the main effect of the ^{6}He breakup comes from the dipole couplings. It is interesting to note that the DPP that corresponds to this calculation consists of a relatively strong imaginary part of long range and relatively weak, repulsive, real part. However, when the dipole couplings were omitted in the calculations, the corresponding DPP consisted of a rather strong repulsive real part and a weak imaginary part. These results confirm the conclusions of Kakuee *et al.* [7], that the dipole couplings with the continuum generate a long-range absorption that suppresses the Coulomb rainbow in the elastic-scattering angular distribution. However, they also show that quadrupole couplings are responsible for the enhancement of the differential cross-section values at backward-scattering angles and have to be taken into account to obtain good agreement with the experimental data at this bombarding energy.

In conclusion, we performed three-body CDCC calculations for ^{6}He elastic scattering from three heavy nuclides at different bombarding energies above the Coulomb barrier. The calculations included couplings with the breakup states of the projectile. We have shown that, by using a simple dineutron model of ^{6}He, one can reproduce very well all the existing experimental data with only one free parameter—the renormalization factor of the dipole couplings with the states from the continuum. This factor was set to the value of 0.5 in the calculations. Such a correction could be related to the

fact that the model $E1$ strength is larger than predicted by more microscopic calculations and found in experiment. The calculations reproduced very well the angular distributions of the elastically scattered ^{6}He as well as the other measured values. They confirm the experimental results that have shown that the cross section for direct ^{6}He breakup in the field of the ^{209}Bi target is significantly smaller than the cross section for the processes of one- and two-neutron transfer. The good agreement with the elastic-scattering data suggests that the most relevant internal degree of freedom of ^{6}He is the coordinate between the alpha particle and the center of mass of the two neutrons. The dineutron model, although giving only a crude description of ^{6}He, takes into account explicitly the excitation of this degree of freedom that occurs during the collision of ^{6}He with different targets. This aspect of the structure of ^{6}He seems sufficient to obtain a satisfactory description of the elastic scattering. The calculations have shown that, although the dipole couplings suppress the Coulomb rainbow, the quadrupole couplings must be included in the calculations to obtain good agreement with the elastic-scattering data at more backward angles.

[1] G. H. Rawitscher, Phys. Rev. C **9**, 2210 (1974).
[2] T. Matsumoto *et al.*, Nucl. Phys. **A738**, 471 (2004).
[3] T. Matsumoto *et al.*, Phys. Rev. C **70**, 061601(R) (2004).
[4] T. Egami *et al.*, Phys. Rev. C **70**, 047604 (2004).
[5] K. Rusek, N. Keeley, K. W. Kemper, and R. Raabe, Phys. Rev. C **67**, 041604(R) (2003).
[6] N. Keeley *et al.*, Phys. Rev. C **68**, 054601 (2003).
[7] O. R. Kakuee *et al.*, Nucl. Phys. **A728**, 339 (2003).
[8] R. Raabe *et al.*, Phys. Lett. **B458**, 1 (1999).
[9] R. Raabe *et al.*, Phys. Rev. C **67**, 044602 (2003).
[10] R. Raabe, Ph.D. thesis, Katholieke Universiteit Leuven, 2001; http://www.fys.kuleuven.ac.be/iks/lisol/research/6he4he/PhDthesis.pdf
[11] K. Rusek, K. W. Kemper, and R. Wolski, Phys. Rev. C **64**, 044602 (2001).
[12] G. Goldring *et al.*, Phys. Lett. **B32**, 465 (1970).
[13] C. M. Perey and F. G. Perey, Phys. Rev. **132**, 755 (1963).
[14] I. J. Thompson, Comput. Phys. Rep. **7**, 167 (1988).
[15] T. Aumann *et al.*, Phys. Rev. C **59**, 1252 (1999).
[16] I. J. Thompson *et al.*, Phys. Rev. C **61**, 024318 (2000).
[17] E. F. Aguilera *et al.*, Phys. Rev. Lett. **84**, 5058 (2000).
[18] K. Rusek, N. Alamanos, N. Keeley, V. Lapoux, and A. Pakou, Phys. Rev. C **70**, 014603 (2004).
[19] J. J. Kolata *et al.*, Phys. Rev. Lett. **81**, 4580 (1998).
[20] J. P. Bychowski *et al.*, Phys. Lett. **B596**, 26 (2004).
[21] P. A. DeYoung *et al.*, Phys. Rev. C **71**, 051601(R) (2005).
[22] I. J. Thompson *et al.*, Nucl. Phys. **A505**, 84 (1989).